Radiative corrections in Yang-Mills Thermodynamics

Dariush Kaviani

IPPP Durham University

1st Symposium on **Analysis of Quantum Field Theory**
9th International Conference of Numerical Analysis and Applied Mathematics
Haldiki, Greece, 19-25 September 2011

23 September 2011

Table of Contents

Table of Contents

Review of Previous Talks

- Ralf's talk
  - Coarsegrained YMT ground state described by adjoint scalar field $\phi(T)$
  - Effective action for top. triv. sector
  - In eff. theory: $SU(2) \stackrel{\phi}{\to} U(1)$, two massive modes, one massless mode
  - Eff. gauge coupling $e(T)$ has pole at T_c and a plateau value of $\sqrt{8}\pi \sim 8.8$ for $T > T_c$
- Markus' talk
  - Loop momenta constraint by $|\phi|$
  - Calculation of polarization tensor $\Sigma^{\mu\nu}$ of the massless mode as example for radiative correction
  - Implementation of constraints on loop momenta
  - Small radiative correction in spite of $e \propto \sqrt{8}\pi \sim 8.8$

Loop expansion in YM-thermodynamics, I

- Pressure p as loop expansion in connected diags: $p = T \log Z/V$
- Connected diags: loop diags. with no external legs

Problem

In a perturbative approach to YM thermodynamics the a priori estimate for the ground state is trivial and leads to the nonconvergence of the small-coupling expansion of the partition function Z.

Cause

The presence of topologically nontrivial fluctuations, which do contribute to the thermodynamics of the YM system in a direct (ground-state estimate) and an indirect (quasiparticle masses) way, is neglected in a perturbative loop expansion due to an essential zero of their weight in the partition function.

Loop expansion in YM-thermodynamics, II

Solution

The effective theory contains an emergent, inert, and adjoint scalar field ϕ which describes the topologically nontrivial part of the ground state.
In the effective theory, thermodynamical quantities (e.g. pressure) are calculated as effective loop expansions about the nontrivial ground state.

Table of Contents

Feynman rules, vertices

- Recall: unitary-Coulomb gauge, which is a completely fixed gauge and thus no Fadddeev-Popov determinants need to be considered and no ghost fields need to be introduced
- 3-vertex:

$$\Gamma^{\mu\nu\rho}_{[3]abc} = e(T)\,(2\pi)^4\delta(p+q+k)\varepsilon_{abc}[g^{\mu\nu}(q-p)^\rho + g^{\nu\rho}(k-q)^\mu + g^{\rho\mu}(p-k)^\nu]$$

- 4-vertex:

$$\Gamma^{\mu\nu\rho\delta}_{[4]abcd} = -ie^2(T)(2\pi)^4\delta(p+q+s+r) [\varepsilon_{fab}\varepsilon_{fbd}(g^{\mu\rho}g^{\nu\sigma} - g^{\mu\sigma}g^{\nu\rho}) + \varepsilon_{fac}\varepsilon_{fdb}(g^{\mu\sigma}g^{\rho\nu} - g^{\mu\nu}g^{\rho\sigma}) + \varepsilon_{fad}\varepsilon_{fbc}(g^{\mu\nu}g^{\sigma\rho} - g^{\mu\rho}g^{\sigma\nu})]$$

Feynman rules, propagators

- Free propagator of massive mode (real time)

$$D^{TLH,0}_{\mu\nu,ab}(k) = -2\pi\delta_{ab}\tilde{D}_{\mu\nu}\delta(k^2 - m^2)\, n_B(|k_0|/T)\,, \quad a, b \in \{1, 2\}$$

  No vacuum propagator for massive modes (see Ralf's talk)

- Free propagator of massless mode (real time)

$$D^{TLM,0}_{\mu\nu,ab}(p) = \delta_{a3}\delta_{b3}\left\{P^T_{\mu\nu}\left[\frac{-\mathrm{i}}{p^2 + \mathrm{i}\epsilon} - 2\pi\delta(p^2)\, n_B(|p_0|/T)\right] + \mathrm{i}\frac{u_\mu u_\nu}{\mathbf{p}^2}\right\}$$

$$P^{00}_T = P^{i0}_T = P^{0i}_T = 0\,, \qquad P^{ij}_T = \delta^{ij} - \frac{p^i p^j}{p^2}$$

Feynman rules, constraints

- The compositeness constrains on loop momenta are (see Markus' talk)

$$
\begin{aligned}
|(p_1 + p_2)^2| &\leq |\phi|^2 \quad (s \text{ channel}) \\
|(p_3 - p_1)^2| &\leq |\phi|^2 \quad (t \text{ channel}) \\
|(p_2 - p_3)^2| &\leq |\phi|^2 \quad (u \text{ channel})
\end{aligned}
$$

- Massive modes propagate on-shell only

$$k^2 = m^2$$

- Momentum of massless mode constraint by $|p^2| \leq |\phi|^2$

Table of Contents

2-loop diagrams

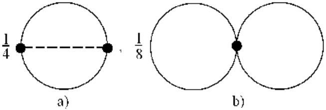

solid (dashed) lines $\leftrightarrow$ massive (massless) modes

$$
\begin{aligned}
\Delta P_a &= \frac{1}{8\mathrm{i}} \int \frac{\mathrm{d}^4 p\, \mathrm{d}^4 k}{(2\pi)^8} \Gamma^{\lambda\mu\nu}_{[3]abc}(p, k, -p, -k) \Gamma^{\rho\delta\tau}_{[3]rst}(-p, -k, p+k) \\
&\quad \times D_{\lambda\rho,ar}(p) D_{\mu\rho,bs}(k) D_{\nu\tau,ct}(-p,-k), \\
\Delta P_b &= \frac{1}{8\mathrm{i}} \int \frac{d^4 p\, d^4 k}{(2\pi)^8} \Gamma^{\mu\nu\rho\delta}_{[4]abcd} D_{\mu\nu,ab}(p) D_{\rho\delta,cd}(k)
\end{aligned}
$$

2-loop diagrams, cntd

Use Feynman rules and carry out the following steps:

- Lorenz and color contractions
- Represent the spatial components of 4 dim. integrals in spherical coordinates
- Integrate over temporal loop momenta using delta functions arising from the thermal parts of the propagators

$$\Rightarrow \Delta P_{a(b)} \simeq e^2 \Lambda^4 \lambda^{-2} \int \prod_{i=1}^{2} dx_i \prod_{i \neq j=1}^{2} dz_{ij} \times \text{Polynomials} \times \text{Bose-factors}$$

2-loop diagrams, constraints

- Potentially noncompact independent loop variables for 2-loop diag are $(p_0, |\mathbf{p}|)$ and $(k_0, |\mathbf{k}|)$.
  Number of potentially noncompact independent loop variables $\tilde{K} = 4$
- The constraints for 2-loop diagrames are
  – on-shellness: $p^2 = k^2 = 4e^2|\phi|^2$
  – compositeness constraints:

$$\left| 4e^2 \pm \sqrt{x_1^2 + 4e^2}\sqrt{x_2^2 + 4e^2} - x_1 x_2 z_{12} \right| \leq \frac{1}{2} \, ,$$

  where $x_1 \equiv \frac{|\mathbf{p}|}{|\phi|}$ and $x_2 \equiv \frac{|\mathbf{k}|}{|\phi|}$
- For 2-loop, we have the total number of constraints

$$K = 1 + 2 = 3$$

- Thus for the 2-loop case we have more noncompact loop variables than constraints: $\tilde{K} > K$
- $\Rightarrow$ noncompact integration region (Markus' talk)

Numerical computings: 2-loop diag. (b) with MC

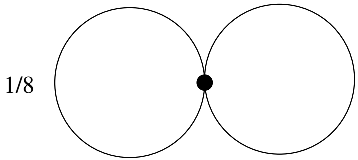

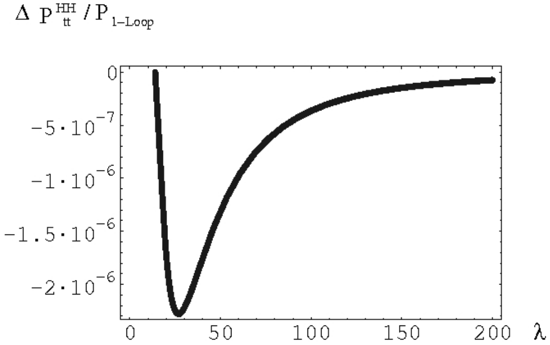

Table of Contents

3-loop diagrams

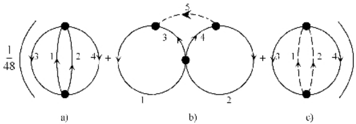

Ir. 3-loop diagrams: Solid (dashed) lines are associated with the propagators of massive (massless) modes

$$\Delta P_a = \frac{1}{48} \int \frac{\mathrm{d}^4 p_1 \mathrm{d}^4 p_2 \mathrm{d}^4 p_3}{(2\pi)^4 (2\pi)^4 (2\pi)^4} \Gamma^{\mu\nu\rho\sigma}_{[4]abcd} \Gamma^{\bar{\mu}\bar{\nu}\bar{\rho}\bar{\sigma}}_{[4]\bar{a}\bar{b}\bar{c}\bar{d}} \times D_{\rho\bar{\rho},c\bar{c}}(p_1) D_{\sigma\bar{\sigma},d\bar{d}}(p_2) D_{\mu\bar{\mu},a\bar{a}}(p_3) D_{\nu\bar{\nu},b\bar{b}}(p_4),$$

$$\Delta P_b = \frac{1}{48} \int \frac{\mathrm{d}^4 p_1 \mathrm{d}^4 p_2 \mathrm{d}^4 p_3}{(2\pi)^4 (2\pi)^4 (2\pi)^4} \Gamma^{\alpha\beta\gamma\lambda}_{[4]hijk} \Gamma^{\mu\nu\rho}_{[3]abc} \Gamma^{\bar{\mu}\bar{\nu}\bar{\rho}}_{[3]\bar{a}\bar{b}\bar{c}} D_{\mu\alpha,ah}(p_1) \times D_{\bar{\mu}\beta,\bar{a}i}(p_2) D_{\gamma\rho,jc}(p_3) D_{\lambda\bar{\rho},k\bar{c}}(p_4) D_{\mu\bar{\nu},b\bar{b}}(p_5)$$

$$\Delta P_c = \frac{1}{48} \int \frac{\mathrm{d}^4 p_1 \mathrm{d}^4 p_2 \mathrm{d}^4 p_3}{(2\pi)^4 (2\pi)^4 (2\pi)^4} \Gamma^{\mu\nu\rho\sigma}_{[4]abcd} \Gamma^{\bar{\mu}\bar{\nu}\bar{\rho}\bar{\sigma}}_{[4]\bar{a}\bar{b}\bar{c}\bar{d}} D_{\rho\bar{\rho},c\bar{c}}(p_1) \times D_{\sigma\bar{\sigma},d\bar{d}}(p_2) D_{\mu\bar{\mu},a\bar{a}}(p_3) D_{\nu\bar{\nu},b\bar{b}}(p_4)$$

3-loop diagrams, general constraints

- Potentially noncompact independent loop variables for ir. 3-loop diags are $(p_0, |\mathbf{p}|)_i$ for $i = 1, 2, 3$.
  Number of potentially noncompact independent loop variables

$$\tilde{K} = 6$$

- The compositeness constrains for ir. 3-loop diags. are

$$\begin{aligned} |(p_1 + p_2)^2| &\leq |\phi|^2 \quad (s \text{ channel}) \\ |(p_3 - p_1)^2| &\leq |\phi|^2 \quad (t \text{ channel}) \\ |(p_2 - p_3)^2| &\leq |\phi|^2 \quad (u \text{ channel}) \end{aligned}$$

- Additional constraints depend on the number of massless and massive propagators in each individual ir. 3-loop diag.

Constraints and compactness: ir. 3-loop diag. (a) and (b)

- We have 3 compositeness constraints due to the s-, t-, u-channels
- In addition to the compositeness constraints, we have the on-shellness conditions:

$$p_1^2 = m^2, \quad p_2^2 = m^2, \quad p_3^2 = m^2, \quad p_4^2 = (p_1 + p_2 - p_3)^2 = m^2$$

- The max. off-shellness of the massless mode in diag. (b) is automatically satisfied by the t-channel due to momentum conservation, $p_5 = p_1 - p_3$
- The total number of constraints for diag. (a) and (b) is

$$K = 3 + 4 = 7$$

- Thus for ir. 3-loop diag. (a) and (b) we have

$$\tilde{K} = 6 < 7 = K$$

$\Rightarrow$ Compact integration region

Constraints and compactness: ir. 3-loop diag. (c)

- As before, we have 3 compositeness constraints over the s-, t-, u-channels
- In addition to the compositeness constraints, the on-shellness relations for the massive modes in diag. (c)

$$p_3^2 = m^2, \quad p_4^2 = (p_1 + p_2 - p_3)^2 = m^2$$

- For diag. (c), we also have the following constraints due to the max. off-shellness

$$|p_1^2| \leq |\phi|^2, \quad |p_2^2| \leq |\phi|^2$$

- The above constraints yield for diag. (c)

$$K = 3 + 4 = 7$$

- Thus for all ir. 3-loop diag. $K = 3 + 4 = 7$ and

$$\tilde{K} < K$$

$\Rightarrow$ Compact or empty integration region

Ir. 3-loop integrations

$$\begin{aligned}
\Rightarrow \Delta P_{a(b)} &\simeq e^4\Lambda^4\lambda^{-2}\sum_{l,m}^{2}\int\prod_{i=1}^{3}dx_i\prod_{i\neq j=1}^{3}dz_{ij}\times\text{Polynomials}\\
&\quad\times\text{Bose-factors}\times\text{delta-functions},\\
\Rightarrow \quad \Delta P_c &\simeq e^4\Lambda^4\lambda^{-2}\sum_{l,m}^{2}\int dy\prod_{i=1}^{3}dx_i\prod_{i\neq j=1}^{3}dz_{ij}\times\text{Polynomials}\\
&\quad\times\text{Bose-factors}\times\text{delta-functions}
\end{aligned}$$

Rescaled constraints: ir. 3-loop diag. (a) and (b)

$$
\begin{aligned}
z_{12} &\leq \frac{1}{x_1 x_2}\left(4e^2 - \sqrt{x_1^2+4e^2}\sqrt{x_2^2+4e^2} + \frac{1}{2}\right) \equiv g_{12}(x_1,x_2)\,, \\
z_{13} &\geq \frac{1}{x_1 x_3}\left(-4e^2 + \sqrt{x_1^2+4e^2}\sqrt{x_3^2+4e^2} - \frac{1}{2}\right) \equiv g_{13}(x_1,x_3)\,, \\
z_{23} &\geq \frac{1}{x_2 x_3}\left(-4e^2 + \sqrt{x_2^2+4e^2}\sqrt{x_3^2+4e^2} - \frac{1}{2}\right) \equiv g_{23}(x_2,x_3)\,.
\end{aligned}
$$

Rescaled constraints: ir. 3-loop diag. (c)

$$
\begin{aligned}
1 &\geq |y_1^2 + y_2^2 - x_1^2 - x_2^2 + 2y_1y_2 - 2x_1x_2z_{12}|\,, \\
1 &\geq |y_2^2 - x_2^2 + 4e^2 - (-1)^l 2y_2\sqrt{x_3^2 + 4e^2} + 2x_2x_3z_{23}|\,, \\
1 &\geq |y_1^2 - x_1^2 + 4e^2 - (-1)^l 2y_1\sqrt{x_3^2 + 4e^2} + 2x_1x_3z_{13}|\,, \\
1 &\geq |y_1^2 - x_1^2|\,, \qquad 1 \geq |y_2^2 - x_2^2|\,,
\end{aligned}
$$

where

$$
\begin{aligned}
y_1 &\equiv \frac{p_1^0}{|\phi|}\,, \\
y_2 &\equiv -y_1 + 2(-1)^l\sqrt{x_3^2 + 4e^2} + (-1)^m f_2(\mathbf{x}, \mathbf{z})\,,
\end{aligned}
$$

and

$$
f_2(\mathbf{x}, \mathbf{z}) \equiv \sqrt{x_1^2 + x_2^2 + x_3^2 + 2x_1x_2z_{12} - 2x_1x_3z_{13} - 2x_2x_3z_{23}}\,.
$$

Monte-Carlo for ir. 3-loop integrations

- Difficulty: ir. 3-loop corrections from diag. (a)-(b) and (c) involve 6- and 7-dim. integrations, respectively
- Deterministic methods for integrations are too time consuming
- Motivation of using MC: MC is a statistical method and much more efficient for such high dim. integrations
- Sample for MC: region of radial loop integration
- Bounding for MC is automatic at 3-loop: compositeness constraints over s-,t- and u-channels
- For diag. (a) and (b), the compositeness constraints determine the region of radial loop integration explicitly
- For diag. (c), the constraints are not fully resolvable as for diag. (a) and (b), and a different method is considered to determine the region of integration

Numerical computings: ir. 3-loop diag. (a) and (b)

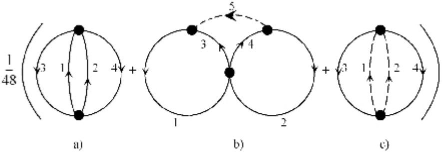

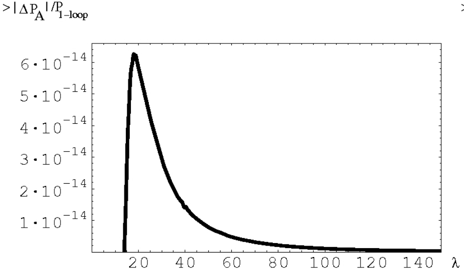

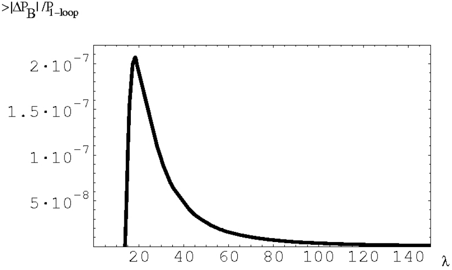

Numerical computings: ir. 3-loop diag. (c)

- For diagram (c) the compositeness constraints are very restrictive and cannot be resolved due to the off-shellness of massless modes
- For diagram (c) the region of radial loop integration is determined by a different method
- Method: a small sampling volume containing only a subset of the integration region is considered
- In this subset a large number of points are chosen randomly for the seven variables
- It is then checked by running millions of tests whether any of these points satisfy the constraints
- No points are found to satisfy all conditions simultaneously
- This continues to hold upon successive enlargement of the sampling volume
- Thus we conclude that the region of integration is empty for diagram (c)
- Ir. diag. (c) has a vanishing contribution!

Hierarchy between 2-loop and 3-loop corrections

- Ir. 3-loop integrations generate hierarchically suppressed contributions to the pressure over the 2-loop contributions:

$$\frac{P_{\text{2-loop}}}{P_{\text{1-loop}}} \leq 10^{-2}$$
$$\frac{P_{\text{3-loop}}}{P_{\text{1-loop}}} \leq 10^{-5}\,\frac{P_{\text{2-loop}}}{P_{\text{1-loop}}} = 10^{-7}$$

- Ir. 3-loop integrations are either compact (ir. diags. (a)-(b)) or empty (ir. diag. (c)) whereas 2-loop integrations are noncompact
- The most striking difference between 2-loop and 3-loop corrections: the contribution from the ir. 3-loop diag. (c) is vanishing; no 2-loop diagram has this property

Relation between pressure and polarization tensor

The polarization tensor is a sum over connected bubble diags. with one internal line of momentum p cut, such that the diag. remains connected, and the two so-obtained external lines amputated

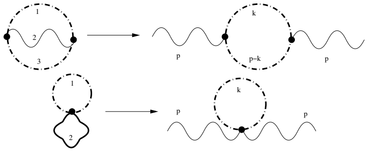

Consequences:

- The hierarchical suppression of 3-loop compared to 2-loop justifies the calculation of the polarization tensor on 1-loop level (as done in Markus' talk).
- The vanishing of a connected bubble diag. due to a zero-measure support for its loop-momenta integrations implies that the associated contribution to a polarization tensor is also nil.

Table of Contents

N-loop diagrams

- Euler-L'Huilliers characteristics: $V - I + L + 1 = 2 - 2g$ (L: # independent loop momenta, I: # internal lines, V: # vertices, g: genus of diagram)
- diag. containing solely (i) V_4 four-vertices, (ii) V_3 three-vertices:

$$(i)\ I = 2V_4 \qquad\qquad (ii)\ I = 3/2V_3\,.$$

- (i): $2V_4$ constraints (propagators) + (at least) $3/2V_3$ constraints (vertices) $\Rightarrow$ total number of constraints $K \geq 7/2V_4$
  (ii): $K = 3/2V_3$ (propagators)
- # of potentially noncompact loop-variables $\tilde{K} = 2L$
- Put together:

$$\frac{\tilde{K}}{K} \leq \frac{4}{7}\left[1 + \frac{1}{V_4}(1-2g)\right]\,, \quad \frac{\tilde{K}}{K} \leq \frac{2}{3}\left[1 + \frac{2}{V_3}(1-2g)\right]$$

The conjecture

- Constraints are inequalities (rather than equalities): $|p^2 - m^2| \leq |\phi|^2$ and $|p^2| \leq |\phi|^2$
- $\tilde{K}/K \leq 1$: compact integration regions (rather than isolated points)

$$\frac{\tilde{K}}{K} \leq \frac{4}{7}\left[1 + \frac{1}{V_4}(1-2g)\right], \quad \frac{\tilde{K}}{K} \leq \frac{2}{3}\left[1 + \frac{2}{V_3}(1-2g)\right]$$

- If $\tilde{K}/K$ is sufficiently smaller than unity, which should be the case for sufficiently large V_4 and/or V_3, then the associated diag. should not contribute (e.g. $g = 0$: $V_4 \geq 2$, $V_3 \geq 6$).

Conjecture

There are only finitely many nonvanishing connected bubble diagrams, provided that all 1PI contributions to the polarization tensor are resummed.

The loop expansion converges rapidly.

The conjecture, evidence

- Integration regions for 2-loop pressure are non-compact, yet $P_{\text{2-loop}}$ is at most 1% of $P_{\text{1-loop}}$
- Integration regions for 3-loop pressure are compact; The modulus of the *dominant* ir. 3-loop contribution, coming from diag. (b), is nearly equal to modulus of the *smallest* 2-loop contribution
- The contribution from the ir. 3-loop diag. (c) is vanishing

Proof?

Your ideas are welcome!

Thank you.